*Kinetics and Catalysis, Vol. 44, No. 4, 2003, pp. 562–571. From Kinetika i Kataliz, Vol. 44, No. 4, 2003, pp. 614–624.*


**HIGHLY ORGANIZED CATALYTIC SYSTEMS**

# Towards a Molecular Understanding of Asymmetric Heterogeneous Catalysis: Hydrogenation of 1-Phenyl-1,2-Propanedione[1]

**E. Toukoniitty, P. Mäki-Arvela, V. Nieminen, T. Salmi, and D. Yu. Murzin**

*Laboratory of Industrial Chemistry, Process Chemistry Group, Åbo Akademi University, Turku, Finland, Fax: +358 2 2154479, e-mail: dmurzin@abo.fi*

Received September 3, 2002

**Abstract**—The present work comprises a detailed investigation of a complex reaction system, revealing features of reaction mechanisms that are general for asymmetric heterogeneous catalysis. Heterogeneous enantioselective hydrogenation of 1-phenyl-1,2-propanedione was studied over cinchonidine modified Pt catalysts producing (*R*)-1-hydroxy-1-phenylpropanone as the main product with an enantiomeric excess (*ee*) of 65% at maximum yield, which could be further increased above 90% due to kinetic resolution. The results of kinetic studies in batch and continuous reactors, catalyst screening and characterization results, as well as quantum chemical calculations, are summarized, and pertinent mechanistic aspects are discussed.

## INTRODUCTION

The synthesis of pure optical isomers is of utmost importance in the production of pharmaceuticals, agrochemicals, fragrances, nutraceuticals, etc. Asymmetric catalysis provides the preferred way for production of optically active compounds from prochiral raw materials. Asymmetric homogeneous and enzymatic catalysts often exhibit a superior (enantio)selectivity; however, the limitations in large-scale industrial production are evident. Modified heterogeneous catalyst are particularly interesting alternatives for large-scale production. The limited examples available have demonstrated that high enantiomeric excesses (*ee* > 95%) exceeding those obtained over existing homogeneous catalysts for the same reaction can be achieved [1, 2]. The principle of modified heterogeneous catalysis is superficially simple: a chiral substance called a modifier is present in the system, and enantioselectivity is obtained due to specific interactions induced by the modifier. However, today the limited understanding of the reaction mechanism has rendered the utilization of heterogeneous modified catalysis to industrially interesting processes difficult.

Supported Pt catalysts modified with cinchona alkaloids have been widely used in the hydrogenation of α-keto esters [2, 3] to corresponding lactates with an *ee* approaching 98%. The hydrogenation of other substrates has been limited [4–6] to minor screening of the system properties. However, for a general understanding of asymmetric induction over modified noble metal catalysts, the extensive investigation of other model systems becomes important. In this work the results obtained using asymmetric dione, 1-phenyl-1,2-propanedione [7–12], have been summarized, and some mechanistic aspect are discussed.

## EXPERIMENTAL

1-Phenyl-1,2-propanedione was hydrogenated in a pressurized autoclave (Parr Instruments, $V = 300$ cm$^3$). The hydrogen pressure and temperature were 1.2–6.5 bar and 0–35°C, respectively. Catalyst was activated prior to the reaction under hydrogen flow for 2 h at 400°C. An *in situ* catalyst modification procedure was adopted, i.e., the degassed solvent, cinchonidine, and the substrate were injected into the reactor, where the activated catalyst was under hydrogen, and the reaction was commenced immediately. The initial concentrations of 1-phenyl-1,2-propanedione and cinchonidine were typically 0.025 mol dm$^{-3}$ and $2.3 \times 10^{-4}$ mol dm$^{-3}$, respectively. Details of the batch reactor experiments have been reported elsewhere [7, 8].

Hydrogenation of 1-phenyl-1,2-propanedione was also carried out in a continuous fixed-bed reactor (10 cm in length and 1.2 cm in internal diameter) at 25°C and 5 bar $H_2$. The knitted fibrous catalyst (5 wt % $Pt/SiO_2$) was placed between stainless steel nets, and glass beads were used as an inert packing material. Prior to the reaction, the catalyst was reduced *in situ* under flowing hydrogen at 400°C for 2 h. The experimental setup and catalyst structure are demonstrated in Fig. 1. Experimental details have previously been reported [12, 13].

[1] This article was submitted by the authors in English.

0023-1584/03/4404-0562$25.00 © 2003 MAIK "Nauka / Interperiodica"

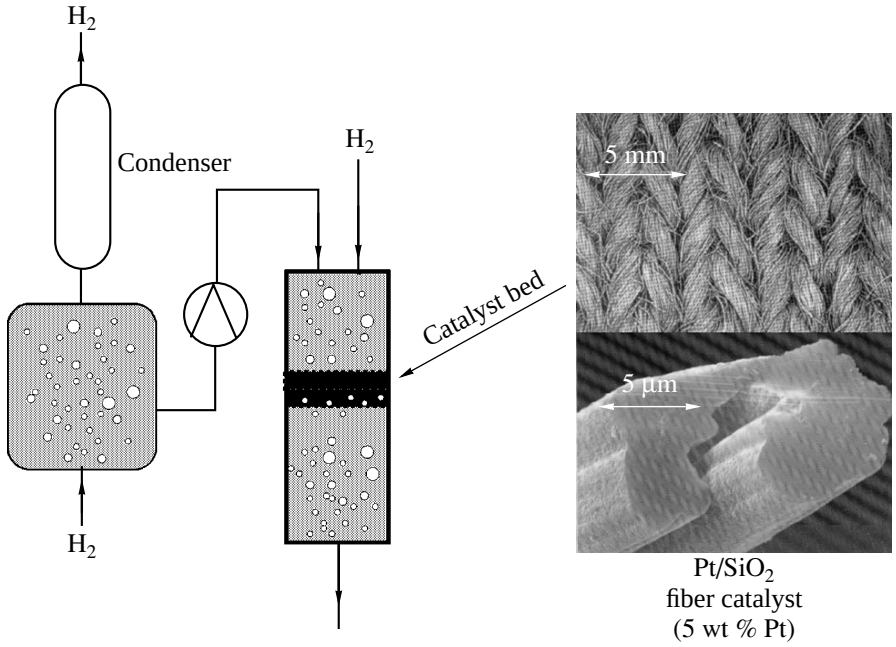


**Fig. 1.** Reactor setup and SEM images of a knitted fibrous catalyst support and a single catalyst fiber.

Collected samples were analyzed with a gas chromatograph. Details of the analysis procedure and identification of the peaks have been published previously [7].

## RESULTS

### *General*

The reaction scheme of 1-phenyl-1,2-propanedione (**A**) hydrogenation is displayed in Fig. 2. The reactant, **A**, has two carbonyl groups, both of which can be hydrogenated. Due to the complexity of the system, consecutive hydrogenation and kinetic resolution of intermediate hydroxyketones, as well as regio-, enantio-, and diastereoselective product formation, are involved.

Cinchonidine was used as a catalyst modifier (**M**, Fig. 2). The vinyl-group (C10-C11, Fig. 2) of cinchonidine hydrogenated under reaction conditions rapidly within the first minutes of reaction converting cinchonidine to 10,11-dihydrocinchonidine (GC-MS conformation) [7]. Therefore, the actual modifier during the main course of reaction was 10,11-dihydrocinchonidine instead of cinchonidine. The main product in hydrogenation of **A** in the presence of cinchonidine was (*R*)-1-hydroxy-1-phenylpropanone (**B**, Fig. 2), a key intermediate in the synthesis of, for example, L-ephedrine [17, 18]. When cinchonine, a near enantiomer of cinchonidine, was used, the main product was (*S*)-1-hydroxy-1-phenylpropanone, **C** [15]. 2-Hydroxy-1-phenylpropanone (**D** + **E**) and diols **G** and **I** were formed in minor amounts under all reaction conditions. The enantiomeric excess of **B** (*ee*) and regioselectivity are defined as follows:

$$ee = \frac{[\mathbf{B}] - [\mathbf{C}]}{[\mathbf{B}] + [\mathbf{C}]} \times 100\%, \quad (1)$$

$$rs = \frac{[\mathbf{B}] + [\mathbf{C}]}{[\mathbf{D}] + [\mathbf{E}]}, \quad (2)$$

where [**B**], [**C**], [**D**], and [**E**] are the concentrations of compounds **B**, **C**, **D**, and **E** (Fig. 2).

### *Qualitative Kinetics*

Kinetic experiments were carried out in the absence of external and internal mass transfer limitations [8]. The effect of hydrogen pressure was negligible. The reaction order with respect to hydrogen was around zero over the pressure range studied (1.2–6.5 bar). The reaction rate, *ee*, and *rs* remained constant while the hydrogen pressure was varied.

The reaction order with respect to the reactant was 0.7 (calculated from the initial hydrogen uptake rates) at different initial concentrations of **A** (0.010–0.025 mol $dm^{-3}$). The regioselectivity remained constant (*rs* = 10) as the reactant (**A**) concentration was varied, whereas *ee* increased slightly with increasing reactant concentration [8]. The increase of *ee* with increasing reactant concentration is in analogy with observations made with α-ketoesters [1], where both racemic and enantioselective hydrogenation exhibited a maximum as a function of the reactant concentration. In present case maxima in *ee* was not yet reached, due to the low substrate concentrations ($c_{max}$ = 0.025 M)

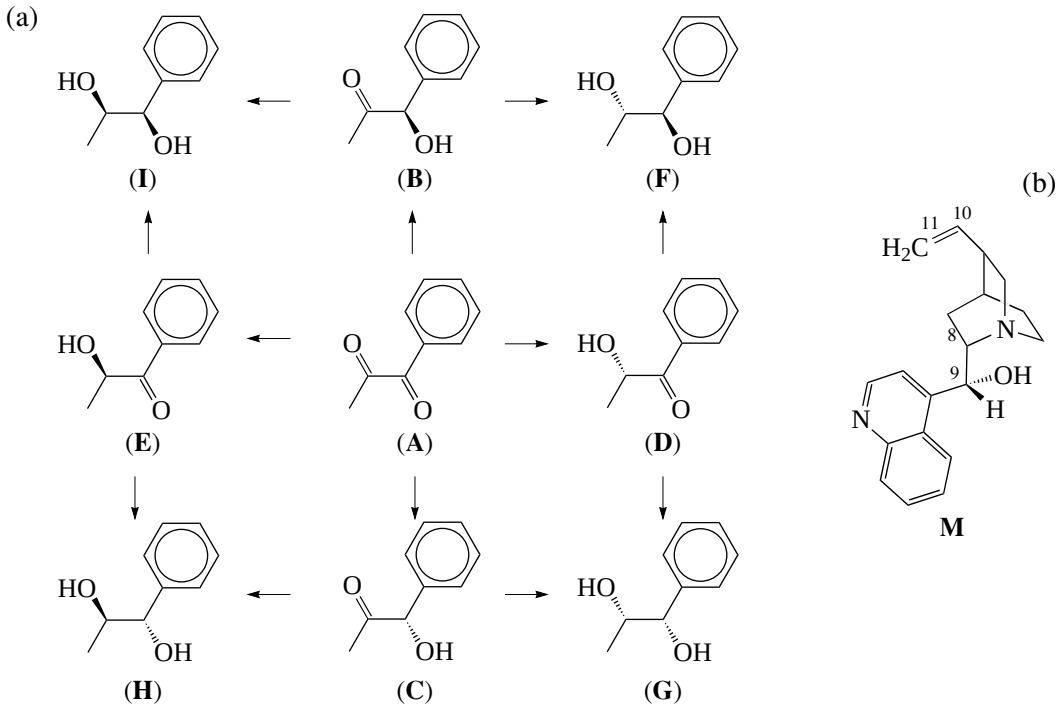


**Fig. 2.** Reaction scheme of 1-phenyl-1,2-propanedione hydrogenation and the catalyst modifier (**M**), cinchonidine. **A**: 1-Phenyl-1,2-propanedione, **B**: (*R*)-1-Hydroxy-1-phenylpropanone, **C**: (*S*)-1-Hydroxy-1-phenylpropanone, **D**: (*S*)-2-Hydroxy-1-phenylpropanone, **E**: (*R*)-2-Hydroxy-1-phenylpropanone, **F**: (1*R*,2*S*)-1-Phenyl-1,2-propanediol, **G**: (1*S*,2*S*)-1-Phenyl-1,2-propanediol, **H**: (1*S*, 2*R*)-1,2-propanediol, and **I**: (1*R*,2*R*)-1-Phenyl-1,2-propanediol.

used, and therefore *ee* increased as the substrate concentration was increased. The concentration of the reactant was not increased above 0.025M because this would cause a shift from an experimentally verified kinetic controlled regime to a hydrogen diffusion controlled regime and thus invalidate the basic prerequisite for a proper kinetic experiment.

The most pronounced effects on catalyst activity, *ee* and *rs*, were observed as the cinchonidine concentration was varied (Fig. 3). The reaction rate varied as a function of the modifier concentration [8]. The maximum rate acceleration of 30% with respect to the absence of modifier was observed at a 1 : 5 molar ratio of cinchonidine-to-surface Pt. When the cinchonidine-to-surface Pt molar ratio was increased above 2 : 1, the overall hydrogenation rate decreased below the racemic hydrogenation rate. The maximum *ee* was observed at the same 2 : 1 cinchonidine-to-surface Pt molar ratio (Fig. 3), which indicates that no significant overall rate acceleration can be observed, as is generally the situation in α-keto ester hydrogenation over the same catalyst. The *rs* had a maximum at around a 1 : 1 cinchonidine-to-surface Pt molar ratio. After the observed maximum values, the reaction rate, *ee*, and *rs* decreased as the concentration of cinchonidine was further increased.

The reaction proceeds further to 1-phenyl-1,2-propanediols (**F-I**, Fig. 2) after extended reaction times. The most abundant diol was **F** in nonpolar media, while the main product was **H** in polar media ($\varepsilon > 15$) [11]. Only small amounts of **G** and **I** were formed.

The reaction temperature had an effect on the overall conversion rate, *ee*, and *rs*. The rate constant increases with increasing temperature following the law of Arrhenius. The apparent activation energy estimated from the initial hydrogen uptake rates was 23 kJ $mol^{-1}$ [14]. The temperature increase from 15 to 35°C resulted in a decrease of *rs* and *ee* from 9.5 to 7.5 and from 65 to 58%, respectively [8]. The dependence of *ee* and *rs* on temperature can be explained by the temperature dependence of the cinchonidine adsorption equilibrium.

Three regions of *rs* and *ee* as a function of the reactant conversion can be distinguished. At low conversions (conversion of **A** < 30%), a transient increase was often observed, which is typical also for α-keto ester hydrogenation [19]. Selectivity between 30 and 90% conversion of **A** was relatively constant (*ee* = 65%, *rs* = 10); however, at conversions exceeding 90%, dramatically increasing *rs* and *ee* were observed, with the *ee* approaching 90%. The increase of *rs* took place both in the absence and presence of a catalyst modifier, whereas the increase of *ee* occurred only when a catalyst modifier was present. (The increase of *ee* was a consequence of kinetic resolution of the intermediate hydroxyketones **B** and **C** to diols.) The increase of *ee* at a high conversion of **A** was achieved at the expense of a lowered yield of **B**. In enantioselective hydrogenation

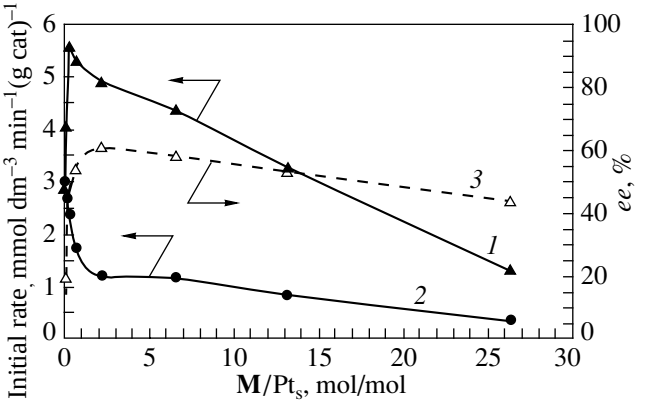


**Fig. 3.** Formation rates of (*1*) (*R*)- and (*2*) (*S*)-1-hydroxy-1-phenylpropanones at different molar ratios of cinchonidine (**M**)-to-surface $Pt_s$ and (*3*) enantiomeric excess (*ee*).

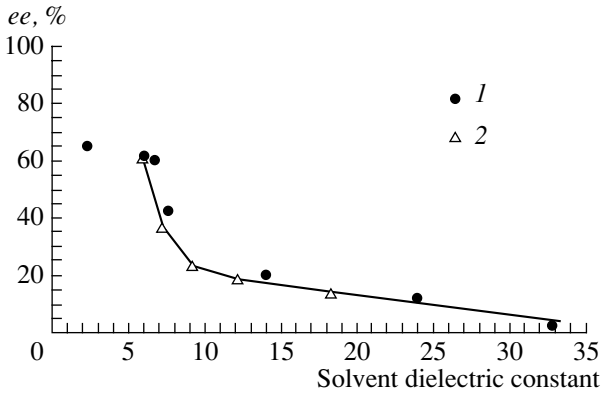


**Fig. 4.** The dependence of enantiomeric excess on solvent dielectric constant using neat solvent and binary ethyl acetate 2-propanol mixtures. (*1*) Neat solvent and (*2*) binary ethyl acetate-2-propanol mixture.

of butane-2,3-dione [4, 5], an analogous kinetic resolution has been reported. The dependence of *rs* on conversion can be explained by the differences in reactivity of **1-OH** and **2-OH**; i.e., **2-OH** reacts faster to diols than **1-OH**, and thus *rs* increases at high reactant conversions.

In the absence and at very low concentrations of cinchonidine, hydrogenation of the phenyl-ring of **A** took place [8, 13]. However, the yield of cyclohexyl derivatives remained low (<10%), and in the presence of higher amounts of cinchonidine, formation of these products was not observed.

### *Solvent Effect*

Enantiomeric excess varied significantly in the different solvents, the *ee* being almost zero in methanol and exceeding 65% in toluene [11]. A highly nonlinear dependence of *ee* on the dielectric constant of the solvent was observed (Fig. 4). In general, relatively nonpolar solvents (toluene, dichloromethane, and ethyl acetate [9]) gave the highest *ee*s. The hydrogenation activity and regioselectivity varied in different solvents, but the initial hydrogenation rate did not correlate with the measured hydrogen solubilities, which can be understood in the light of the zero order dependence of the reaction rate on hydrogen pressure. The measured hydrogen solubility [11] decreased with an increasing solvent dielectric constant. The *rs* did not exhibit strong dependence on the solvent dielectric constant [11].

Interestingly, the product distribution among the diols varied in different solvents. The main product in nonpolar solvents was **F**, whereas **H** was the dominating diol in polar solvents. In nonpolar media, **B** reacted faster, yielding an excess of **F**, and in polar solvents **C** reacted faster, resulting in an excess of **H** [11].

In the present case, the inferior enantioselectivity in alcoholic solvents was attributed to the solvent's ability to interact with the catalyst modifier via hydrogen bonding, similar to the way that substrate and modifier interact, thus preventing enantiospecific interaction between the catalyst modifier and reactant and resulting in decreased enantioselectivity.

Cinchonidine exhibits a rich conformational behavior: at room temperature six different conformers have been recognized consisting of two "Closed" conformers and four "Open" conformers. This complex liquid-phase equilibrium varies as a function of the solvent dielectric constant [20]. However, solvent dependence of *ee* cannot be attributed solely to the liquid-phase concentration of the Open(3) conformer [20], as has been proposed for hydrogenation of ketopantolactone over an analogous modifier catalyst. In [11] the dielectric constant dependence was taken into account by applying the transition state theory and the Kirkwood treatment, which accounts for the effects of the solvent dielectric constant on the rate constant. The model developed was able to predict the behavior of the system as a function of the solvent dielectric constant, and a good description of both *ee* and *rs* was obtained [11].

### *Catalyst Selection, Pretreatment and Role of Oxygen*

Commercial 5 wt % $Pt/Al_2O_3$ catalysts (Johnson Matthey 94 and Strem Chemicals, 78-1660), which have a relatively large average Pt particle size (2.5 nm, Strem) and low dispersion (40%, Strem) gave the highest *ee*s and *r*ss in the hydrogenation of **A**. In prepared $Pt/Al_2O_3$ catalysts, an increasing Pt particle size correlated with an increasing *ee* [9] (Fig. 5). The best catalyst had an average Pt particle size of 4.0 nm and dispersion of 25%. As different $Pt/SiO_2$ catalysts were screened, an optimum dispersion of 27% and average Pt particle size of 3.8 nm was found to give the highest activity and enantioselectivity [12] (Fig. 6). Deviations from the optimum resulted in a decrease in both reaction rate and *ee*. Figure 5 demonstrates clearly that there is an optimum Pt particle size, around 2–4 nm, independent of

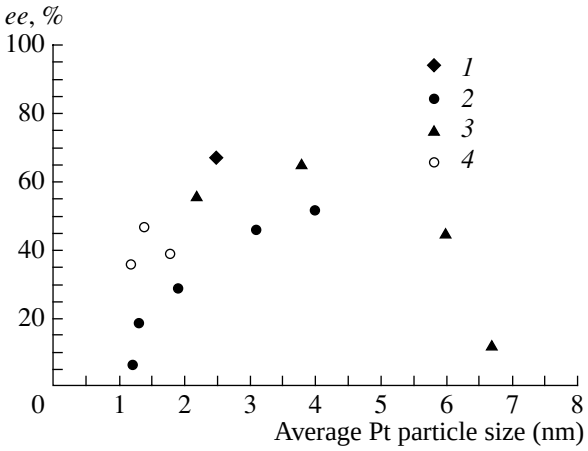


**Fig. 5.** Enantiomeric excess (*ee*) at 50% reactant conversion as a function of average Pt particle size of different Pt catalysts. (*1*) Commercial $Pt/Al_2O_3$ (Strem Chemicals), (*2*) $Pt/Al_2O_3$ prepared from an $H_2PtCl_6$ precursor, (*3*) $Pt/SiO_2$ prepared from an $H_2PtCl_6$ precursor and (*4*) $Pt/Al_2O_3$ prepared from a $Pt(NO_3)_2$ precursor.

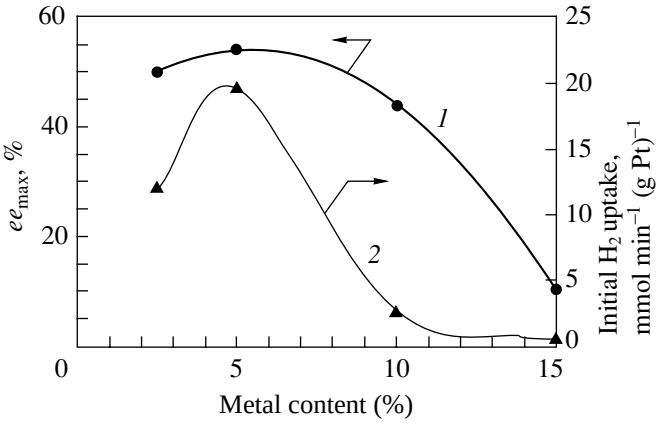


**Fig. 6.** The maximum enantiomeric excess (*ee*) (*1*) and initial hydrogen uptake rate (*2*) as a function of $Pt/SiO_2$ catalyst metal content.

the support and metal precursor used for catalyst preparation, which gives the highest *ee*. The particle size measurement in Fig. 5 was based on hydrogen chemisorption, and all the experiments were carried out with ethyl acetate as the solvent. The characteristic features of the optimal catalyst are in line with the observation made using α-keto esters as well [3].

The catalyst pretreatment also influences the selectivity and activity. The effect of the catalyst reduction temperature was studied over the commercial $Pt/Al_2O_3$ catalyst (Strem) [10]. For maximum *ee* and reaction rate, a catalyst reduction temperature of about 400°C was necessary to obtain a metal surface free of organic impurities.

The small amounts of dissolved oxygen present in the reactant solution were found to influence the reaction rate and *ee* [10]. This effect became clear by injecting oxygen into the reactor through the injection loop [10]. A lower reaction rate and *ee* were observed under anaerobic conditions. Furthermore, trace quantities of oxygen, as well as other impurities, which were removed by solvent distillation, had a beneficial effect on the enantiodifferentiation (Fig. 7) and hydrogenation rate [10]. Similar observations have been made in ethyl pyruvate hydrogenation over a cinchonidine modified $Pt/SiO_2$ catalyst [21], where anaerobic conditions resulted in a low *ee* and reaction rate.

### *Quantum Chemical Calculations*

Theoretical calculations (Hartree–Fock approximation, Möller–Plesset perturbation, and Density Functional Theories) were used in order to increase the molecular level knowledge of the system [16]. The calculations provided explanation for the origin of regioselectivity and also gave valuable information about the structure and conformation of the reactant (Fig. 8). The effect of the solvent on the reactant conformation was accounted for by the polarized continuum model [11]. The solvent had only a minor effect on the reactant conformation. In vacuum and when the solvent effect was included, the reactant adopted s-*trans* conformation where the C=O group 1 and the phenyl ring were coplanar (Fig. 8). The delocalization of electrons between C=O group 1 and the phenyl ring resulted in reduced C1=O1 bond strength and thereby led to a higher hydrogenation rate and regioselectivity. Regioselectivity was further increased in the presence of cinchonidine due to analogous substrate–modifier interactions, which were responsible for enantioselectivity as well. Currently, calculations about the possible reactant–modifier diastereomeric complexes involved in enantiodifferentiation interaction are being carried out. Based on preliminary results, open(3) conformation of the modifier and hydrogen-bonding type interaction (N…H…O=C) between cinchonidine and the reactant are important, which is in accordance with the previous results obtained for α-keto esters.

## CONTINUOUS HYDROGENATION AND TRANSIENT EXPERIMENTS

Fixed bed experiments were carried out over an optimized (metal content and surface area [12]) fibrous $SiO_2$ supported catalyst, which has a low pressure drop and shorter diffusion distance (<5 μm) compared to conventional catalyst pellets (Fig. 1). The catalyst fibers were knitted and thus could be easily introduced into the reactor. In enantioselective hydrogenation, continuous operation has received only minor attention [22, 23] and the majority of the experiments have been carried out in batchwise-operated reactors. In preliminary experiments the performance of the optimized catalyst was encouraging in continuous operation [12]. High conversion of **A** and comparable selectivities to batch

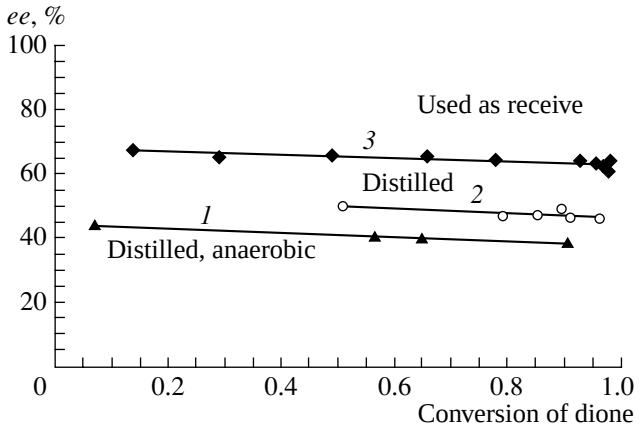


**Fig. 7.** Effect of oxygen. The enantiomeric excess (*ee*) using a distilled solvent under anaerobic conditions (*1*), using a distilled solvent that has been in contact with air (*2*), and using a solvent and reactant as received in contact with air (*3*).

operation were obtained (Fig. 9). Furthermore, the transient behavior of the system and the possibility of evaluating catalyst deactivation make continuous hydrogenation a viable tool for mechanistic studies as well.

### *Transient Behavior of Selectivity*

The initial transient period of *ee* was proportional to space time [16] (Fig. 10), which correlated with the amount of modifier passed over the catalyst. This supports the assumption that the modifier adsorption on the catalyst surface plays a central role. The same steady-state *ee*s were achieved regardless of the differences in transient behavior. The steady-state *ee*s were also independent of the reactant concentration and catalyst mass used. However, the steady-state *ee* varied with different modifier concentrations from 39 to 55%. As expected, in the absence of the modifier, no enantioselectivity was observed. Experiments carried out by stopping and starting the modifier flow revealed that a continuous feeding of the modifier was necessary to maintain a steady-state *ee*. Similar observations have been reported for α-keto ester hydrogenations [22]. The catalyst premodification experiments support the hypothesis that the transient behavior of *ee* was caused by the modifier adsorption. As the catalyst was premodified, the initial *ee* was very high (60%) but decreased with increasing time-on-stream due to desorption of the cinchonidine from the catalyst surface.

In the second hydrogenation step, the $ee_2$ of **F** (defined as $ee_2 = (\mathbf{F} - \mathbf{H})/(\mathbf{F} + \mathbf{H})$) exhibited analogous behavior on the modifier concentration as the *ee*; i.e., it increased along with an increased cinchonidine concentration [12, 13]. This supports the involvement of modifier–reactant interactions in the second hydrogenation step as well.

Regioselectivity also exhibited an interesting transient period [13]. Development of *rs* with increasing modifier coverage could be observed, which was analogous to the development of *ee*. This was in accordance with the batch reactor experiments, where *rs* had a maximum as a function of modifier concentration.

### *Transient Behavior of Phenyl-Ring Hydrogenation*

Cyclohexyl products were formed at the beginning of the reactor operation [13]. The amount of cyclohexyl products decreased with increasing time-on-stream, and the decrease was proportional to the modifier concentration (Fig. 11), leading to a complete disappearance of the cyclohexyl products. In the absence of the modifier, the formation of cyclohexyl products attained a steady-state value greater than zero (Fig. 11). An analogous effect became evident also when the space-time was varied. Therefore, it might be that the space demanded by the strongly adsorbed modifier prevents flat phenyl ring adsorption and thereby formation of cyclohexyl products. This also indicates that the adsorption mode of the reactant might be different in the presence and absence of cinchonidine.

### *Catalyst Deactivation*

Catalyst deactivation was observed during continuous operation [12, 13]. The deactivation could be observed both in the hydrogenation of the phenyl-ring and in the hydrogenation of the carbonyl groups of **A**.

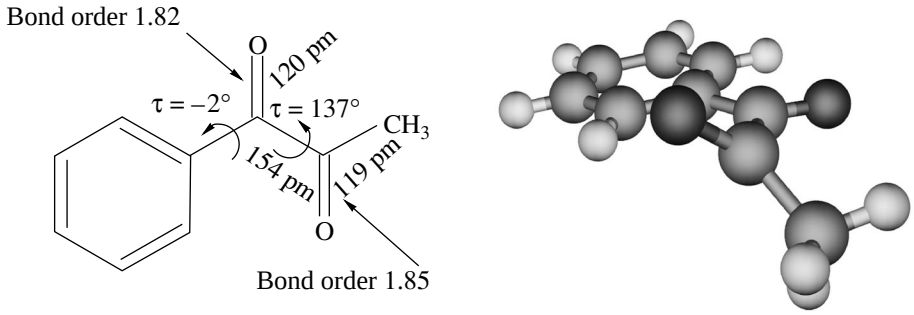


**Fig. 8.** The Hartree–Fock (HF) optimized structure of 1-phenyl-1,2-propanedione in vacuum (right) and selected bond orders, torsion angles (τ), and bond lengths (left).

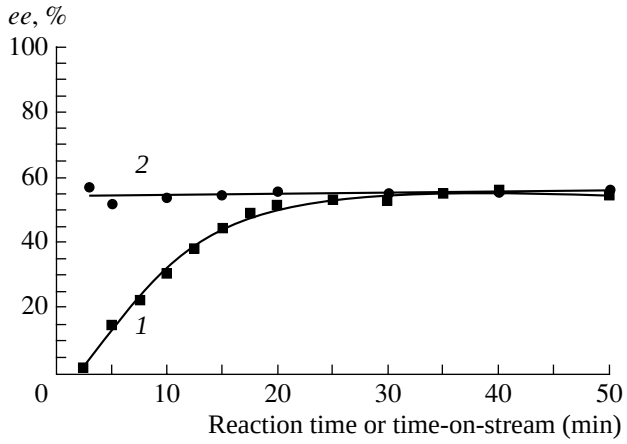


**Fig. 9.** A comparison of the enantiomeric excesses (*ee*) in a continuous fixed bed reactor (*1*) and in a batch reactor (*2*).

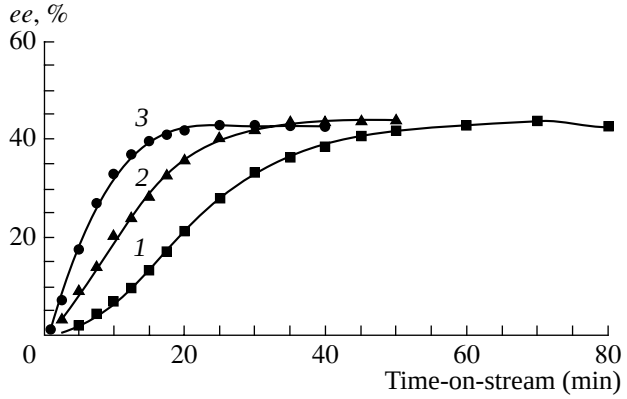


**Fig. 10.** The effect of space-time on the (a) enantiomeric excess (*ee*). Inlet concentrations of **A** and **M** were $c_{0A}$= 0.025 mol dm$^{-3}$ and $c_{0\mathbf{M}} = 10 \times 10^{-5}$ mol dm$^{-3}$, respectively. Symbols: space-time (*1*) 44 s, (*2*) 30 s, and (*3*) 22s.

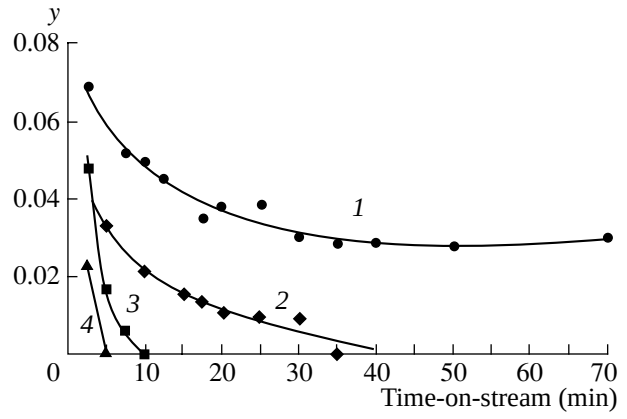


**Fig. 11.** The effect of modifier concentration on the yield of cyclohexyl products. Symbols: (*1*) no modifier, (*2*) 3.4, (*3*) 10, and (*4*) $34 \times 10^{-5}$ mol dm$^{-3}$ of modifier (**M**).

The concentrations of the modifier did not affect the deactivation behavior. Also the role of the solvent, ethyl acetate, could be excluded and the origin of catalyst deactivation could be limited to the reactant (**A**). The role of impurities in the reactant as the origin of deactivation could be excluded based on experiments with purified and unpurified reactant. Therefore, it was concluded [13] that the reactant is either decomposing on the catalyst or just strongly adsorbs in the pores of the catalyst, causing the observed deactivation. The effect of deactivation on the *ee* was minor. The deactivation influenced mainly the overall hydrogenation activity, and not the *ee*. It should be kept in mind that analogous deactivation takes place in batch reactors; however, the interpretation of deactivation is much more difficult compared to continuous operation.

## REACTION MECHANISM

The enantiodifferentiation mechanism over cinchona alkaloid-modified Pt catalysts has been, until very recently, evaluated solely based on ethyl and methyl pyruvates, which makes the utilization of other substrates desirable. Recent reviews can be consulted in order to get an overall idea of the problems and consensus involved [3].

The model reaction exhibited features that were analogous to the well-studied α-keto esters; namely, the optimum catalyst properties, the effect of dissolved oxygen, and the solvent effects were very similar. However, the novel features were related to the origin of enantioselectivity, the lack of overall rate acceleration, and regioselectivity.

In the presence of cinchonidine, a negligible overall rate acceleration compared to racemic hydrogenation was observed, and yet an *ee* of 65% was maximally obtained. This is a specific feature of 1-phenyl-1,2-propandione hydrogenation and should not be overlooked. For other α-keto esters, a pronounced overall rate acceleration, as well as increased production rates of *both enantiomers* in the presence of cinchonidine, has been reported [5, 24], with the exception of ethylbenzoyl formate, for which no correlation was found between the rate and enantioselectivity [25]. The origin of enantioselectivity in the hydrogenation of α-keto esters over a cinchonidine modified catalyst has been the significantly more increased formation rate of the (*R*)-enantiomer with respect to an increased formation rate of the (*S*)-enantiomer, and this has long been taken as a fundamental feature of the cinchona alkaloid modified catalysts. However, in 1-phenyl-1,2-propanedione hydrogenation, the formation rate of the (*R*)-enantiomer (**B**) was increased in the presence of cinchonidine, whereas the formation rate of the (*S*)-enantiomer (**C**) was suppressed compared to racemic hydrogenation, thus providing a high *ee* (Fig. 3).

A maximum *ee* was observed at around a 2 : 1 cinchonidine-to-surface Pt molar ratio, after which the *ee*

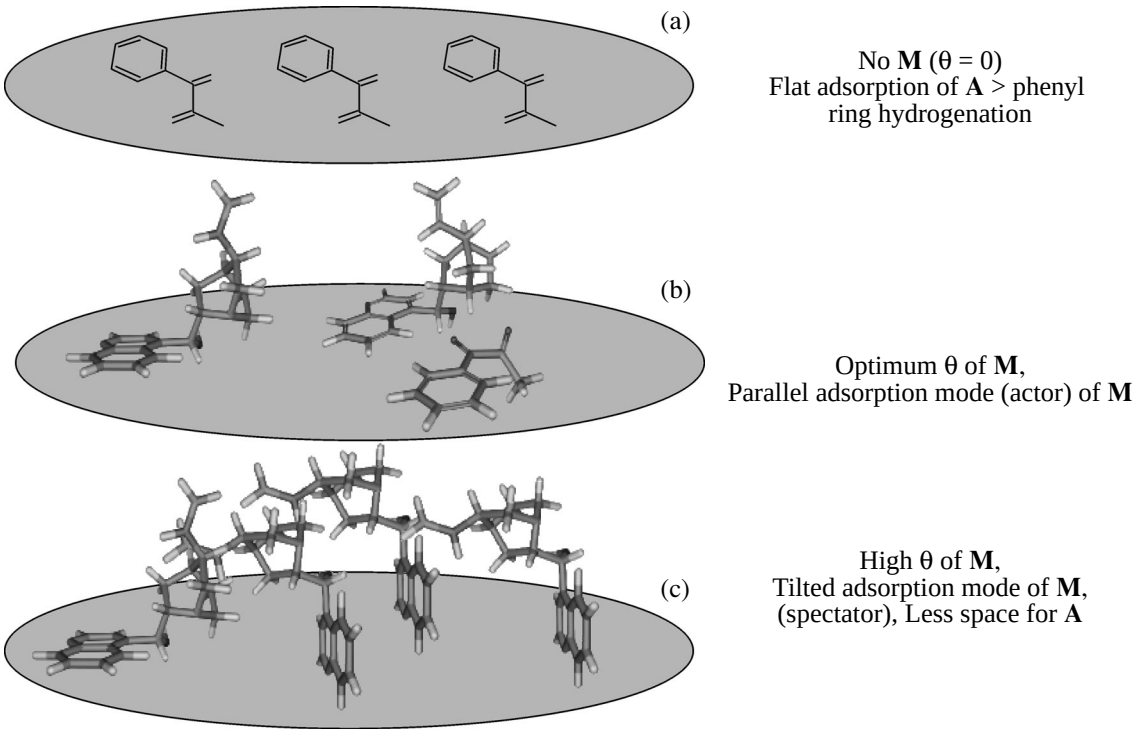


**Fig. 12.** Schematic representation of the hydrogenation mechanism of **A** in the absence of a modifier (top), under optimum coverage of the modifier (middle), and with a large amount of modifier (bottom).

started to decrease with increased cinchonidine concentration (Fig. 3) [8]. An explanation for the decrease of the rate could be the change of the adsorption mode [26, 27] of the modifier and/or the reactant as a function of the surface coverage in such a way that specific enantiodifferentiating interactions are no longer possible. The coverage dependent adsorption modes of reactant and modifier were used as a basis for a quantitative kinetic model, which explained the kinetics observed [8].

In the absence of a modifier, *rs* could be explained by the intrinsic differences between the two reacting carbonyl groups of **A**, which result in a favorable reduction of the carbonyl group in position 1. The over twofold enhancement of the *rs*, due to the small amounts of the modifier added, was analogous with the *ee* exhibiting a similar dependence on the modifier concentration. Therefore, the enhancement of the *rs* could most plausibly be explained by analogous substrate–modifier interactions on the catalyst surface that are also responsible for the enantiodifferentiation and result in an enhancement of *rs*.

Based on detailed kinetic experiments, a quantitative kinetic model was constructed that was able to explain the observed kinetic regularities. The maxima in selectivity were accounted for by introducing coverage dependent adsorption modes of cinchonidine. The parallel adsorption mode was assumed to be the complex forming actor species in enantioselective hydrogenation, while the tilted adsorption mode was assumed to be the spectator species responsible for the decline of activity and selectivity at high concentrations of cinchonidine. For the reactant two adsorption modes were used, representing adsorption via carbonyl group 1 and 2. The derivation of the kinetic equations and parameter estimation procedure have been reported in [8].

In Fig. 12 the present status of the reaction mechanism is presented in a schematic way. In the absence of a modifier, the reactant (**A**) adsorbs mainly in parallel s-*trans* conformation, which is the energy minimized reactant conformation in all solvents. The phenyl ring adsorbs also parallel to the catalyst plane (Fig. 12, top). The flat adsorption mode results in the formation of cyclohexyl products via phenyl ring hydrogenation, as well as other products (Fig. 3) via carbonyl group hydrogenation. No enantiodifferentiation is involved.

In Fig. 12 (middle) the situation represents the optimum coverage of cinchonidine in Open(3) conformation. The fraction of possible Closed conformer of cinchonidine has not been illustrated as it is assumed to be a spectator conformation in enantiodifferentiation. The modifier in Open(3) conformation adsorbed in parallel form is believed to be the actor species in enantiodifferentiation. The substrate–modifier interaction on the catalyst surface results in excess formation of the (*R*)-enantiomer, **B**. Furthermore, the adsorption mode of **A** is no longer totally flat, and therefore phenyl ring hydrogenation does not readily proceed. The theoretical calculations support the assumption that the reactant also adopts s-*cis* conformation, which seems to be energetically favored over the s-*trans* conformation in

the substrate–modifier complex. In kinetic modeling [8] it was assumed that the reactant adopts two adsorption modes, which correspond to the hydrogenation of carbonyl groups of **A**, thus accounting for regioselectivity.

In Fig. 12 (bottom), the situation after the maximum in rate, *ee*, or *rs* has been reached is illustrated. The modifier adopts a tilted adsorption mode, which is assumed to be a spectator species. The tilted form of modifier merely occupies the active Pt surface, thus reducing the overall activity. The lower coverage of the active modifier form (parallel mode) causes reduced *ee* and *rs*.

The above described mechanistic scheme is simplified and should be regarded as a qualitative representation. However, it can account for some of the characteristic features of hydrogenation of **A**, namely, the cyclohexyl product formation and maximum in *ee*, rate, and *rs*. Indirectly, the effect of the solvent can be accounted for by the altered Open/Closed conformational equilibrium and competition between the alcoholic solvent and the reactant on the active form of the modifier. The optimum Pt particle size effect can be understood in the light of the space requirement of the bulky substrate–modifier complex, which sets the lower limit for Pt particle size.

## CONCLUSIONS

Asymmetric synthesis using a modified heterogeneous catalyst has a vast potential in the increasing production of optically pure chemicals.

In the present study, a multidisciplinary approach was applied to investigate heterogeneous enantioselective hydrogenation of 1-phenyl-1,2-propanedione over cinchonidine modified Pt catalysts. This complex reaction enables one to address regioselectivity and enantioselectivity in consecutive hydrogenation steps, thus revealing the features of reaction mechanisms that are general for asymmetric heterogeneous catalysis. Over 70% yields of the main product (*R*)-1-hydroxy-1-phenylpropanone were achieved with high enantiomeric excesses (*ee*) exceeding 65%. However, the *ee* was increased further to about 90% at the cost of a decreased yield of the main product due to kinetic resolution.

1-Phenyl-1,2-propanedione hydrogenation exhibited novel features for cinchona alkaloid-modified Pt catalysts. The overall rate acceleration induced by the modifier was negligible. The high *ee* obtained in the presence of a catalyst modifier was a result of the suppressed formation rate of the (*S*)-enantiomer accompanied by an increased production rate of the main product, the (*R*)-enantiomer.

The dependence of *ee* on the dielectric constant could not solely be attributed to the abundance of the Open(3) conformer of cinchonidine in the liquid phase. The dielectric constant dependence was taken into account by applying the transition state theory and the Kirkwood treatment, which accounts for the effects of the solvent dielectric constant on the rate constant.

An optimized knitted silica fiber-based catalyst was tested under continuous operation conditions. Such operation showed a very rich transient behavior of the system, which further improved our mechanistic understanding of the reaction. The catalyst deactivation during the continuous operation was modeled.

In the kinetic models, a dual-site approach was utilized taking into account simultaneous reaction on modified and racemic sites of the catalyst. Further developments were made including coverage adsorption modes of the modifier and the reactant. The advanced kinetic model gave a good description of experimentally observed kinetics.

## REFERENCES

1. Izumi, Y., *Adv. Catal.*, 1983, vol. 32, p. 215.
2. Blaser, H.-U., Jalett, H.-P., and Wiehl, J., *J. Mol. Catal.*, 1991, vol. 68, p. 215.
3. Baiker, A., *J. Mol. Catal. A: Chemical*, 2000, vol. 163, p. 205 (and references therein).
4. Slipszenko, I., Griffiths, S., Johnston, P., *et al.*, *J. Catal.*, 1998, vol. 179, p. 267.
5. Studer, M., Okafor, V., and Blaser, H.U., *Chem. Commun.*, 1998, p. 1054.
6. Studer, M., Burkhardt, S., and Blaser, H.U., *Chem. Commun.*, 1999, p. 1727.
7. Toukoniitty, E., Mäki-Arvela, P., Kuzma, M., *et al.*, *J. Catal.*, 2001, vol. 204, p. 281.
8. Toukoniitty, E., Ševčíková, A., Mäki-Arvela, P., *et al.*, *J. Catal.*, (in press).
9. Toukoniitty, E., Mäki-Arvela, P., Kalantar Neyestanaki, A., *et al*., *Stud. Surf. Sci. Catal*., 2000, vol. 130, p. 3363.
10. Toukoniitty, E., Mäki-Arvela, P., Nunes Villela, A., *et al.*, *Catal. Today*, 2000, vol. 60, p. 175.
11. Toukoniitty, E., Mäki-Arvela, P., Kuusisto, J., *et al.*, *J. Molec. Catal. A: Chem.*, (in press).
12. Toukoniitty, E., Mäki-Arvela, P., Kalantar Neyestanaki, A., *et al.*, *Appl. Catal. A: General*, 2001, vol. 216, p. 73.
13. Toukoniitty, E., Mäki-Arvela, P., Kalantar Neyestanaki, A., *et al.*, *Appl. Catal. A: General*, 2002, vol. 235, p. 125.
14. Toukoniitty, E., Mäki-Arvela, P., Wärna, J., *et al.*, *Catal Today*, 2001, vol. 66, p. 411.
15. Toukoniitty, E., Mäki-Arvela, P., Sjöholm, R., *et al.*, *React. Kinet. Catal. Lett.*, 2002, vol. 75, p. 21.
16. Toukoniitty, E., Mäki-Arvela, P., Nieminen, V., *et al.*, *Catal. Org. React*, (in press).
17. Gala, D., DiBenedetto, D., Clark, J., *et al.*, *Tetrah. Lett.*, 1996, vol. 37, p. 611.

18. Shukala, V.B. and Kulkarni, P.R., *World J. Microbiol. Biotech.*, 2000, vol. 16, p. 499.
19. Blaser, H.-U., Jalett, H.-P., Garland, M., *et al.*, *J. Catal.*, 1998, vol. 173, p. 282.
20. Bürgi, O. and Baiker, A., *J. Am. Chem. Soc.*, 1998, vol. 120, p. 129.
21. Simons, K.E., Meheux, P.A., Griffiths, S.P., *et al.*, *Reel. Trav. Chim. Pays-Bas*, 1994, vol. 113, p. 465.
22. Künzle, N., Hess, R., Mallat, O., *et al.*, *J. Catal.*, 1999, vol. 186, p. 239.
23. Meheuk, P., Ibbotson, A, and Wells, P., *J. Catal.*, 1991, vol. 128, p. 387.
24. Wells, P.B., and Wilkinson, A.G., *Topics Catal.*, 1998, vol. 5, p. 39.
25. Sutyinszki, M., Szöri, K., and Bartok, M., *Catal Commun.*, 2002, vol. 3, p. 125
26. Ferri, D. and Bürgi, T., *J. Am. Chem. Soc.*, 2001, vol. 123, p. 12074.
27. Ferri, D., Bürgi, O., and Baiker, A., *Chem Commun.*, 2001, p. 1172.